Symbol-Scaling based Constructive Interference Waveform Design for ISAC Systems

Yiran Wang[1], Xiaoyan Hu[1], Ang Li[1], Kai-Kit Wong[2], Kun Yang[3]
[1] School of Information and Communications Engineering, Xi'an Jiaotong University, Xi'an, China
[2] Department of Electronic and Electrical Engineering, University College London, London, UK
[3] School of Computer Science and Electronic Engineering, University of Essex, Colchester, UK
{yiranwang}@stu.xjtu.edu.cn, {xiaoyanhu, ang.li.2020}@xjtu.edu.cn, {kai-kit.wong}@ucl.ac.uk, {kunyang}@essex.ac.uk

***Abstract*—The constructive interference (CI) based symbol-level precoding (SLP) design for integrated sensing and communication (ISAC) systems is investigated in this paper. The minimum communication scaling factor among the users is maximized under radar performance constraint and power constraint through optimizing the transmit signal. In order to solve the proposed optimization problem, two groups of approximate feasible domains are adopted to transform the optimization problem into convex. The simulation results show that the proposed SLP design based on symbol scaling has significant advantages in enhancing the communication performance under the condition that the radar performance satisfy the requirements. And compared with the previous SLP schemes in ISAC system, the computational complexity of the proposed schemes can be reduced significantly.**

***Index Terms*—Symbol scaling, integrated sensing and communication (ISAC), constructive interference (CI), symbol-level precoding (SLP).**

I. Introduction

The rapid growth of wireless services makes spectrum resources scarce. A large portion of the available spectrum of the radar band can be shared with various communication systems. Spectrum sharing between radar and communication systems is consistent with the continuous fusion of integrated sensing and communication (ISAC) [1], [2], which has triggered massive research on coexistence, cooperation and joint design of these two functions [3].

Recently, many researchers have focused on the design of transmit beamforming in multiple-input multiple-output (MIMO) ISAC systems, optimizing the transmit precoding matrix through different radar and communication metrics [4]–[10]. MIMO architecture is widely used in ISAC systems to provide waveform diversity for radar target detection [11], beamforming gain and spatial multiplexing for multi-user communications.

The transmit waveform designs mentioned above [4]–[10] are all conventional block-level precoding (BLP). However, since conventional BLP designs employ performance metrics mainly based on the second-order statistics (e.g., SINR and MSE) to optimize the average transmit beampattern, the radar sensing performance can be guaranteed only when the number of transmitted symbols is sufficiently large. As a result, the instantaneous transmit beampatterns in different time slots might have significant distortions, which causes severe performance degradation on target detection and parameter estimation if only a limited number of samples are collected. In light of the shortcomings for BLP, symbol-level precoding (SLP) technology is further adopted in ISAC systems.

Unlike the conventional BLP, SLP is a non-linear and symbol-dependent approach, which optimizes each instantaneous transmitted vector based on the specific symbols to be transmitted, rather than simply eliminates MUI at the symbol level [12]. From the communication perspective, SLP can exploit the symbol information to convert harmful MUI into constructive components, i.e., constructive interference (CI), to reduce the symbol error rate (SER) and perform more reliable multi-user communications. From the radar perspective, the instantaneous transmit beampattern in each time slot can be carefully designed and a well-formed beampattern can be guaranteed with a limited number of waveform samples.

In previous work [13], the transmit vectors for CI-based SLP (CI-SLP) are optimized to minimize the squared error between the obtained and the desired beampattern, subject to CI constraints for communications and power constraints. This work confirms the significant advantage of SLP in enhancing the communication performance over conventional BLP, but the complexity of the optimization problem is difficult to accept due to the non-convex nature of the objective function. In addition, [14] utilizes space-time adaptive processing (STAP) and CI-SLP to implement MIMO ISAC. This scheme shows better performance in the presence of strong signal-dependent clutter. In [15], the authors investigate the SLP-based low-range-sidelobe waveform design for an MIMO-OFDM ISAC system, and the simulation results reveal the performance improvement of radar ranging. All these work take radar performance as the objective function of optimization problems. The non-convex objective function make the optimization problem difficult to solve directly and the iterative methods are resorted to provide solvable solutions which require a large number of iterations and make the computational complexity of these schemes difficult to accept. On the other hand, under high communication requirements, the infeasible probability of these schemes will also increase. In other words, the communication performance of these CI-SLP ISAC schemes is limited. In view of these shortcomings, we adopt the symbol-scaling metric in CI-SLP ISAC system and take the communication performance as the objective function of optimization problem, taking the radar

performance as a necessary constraints, which has not been previously investigated in the literature.

The contributions of this paper can be summarized as follows:

• We initially propose a symbol-scaling based CI-SLP design in ISAC system. The minimum communication scaling factor among the communication users is maximized while satisfying the radar target illumination power requirement and total power budget constraint.

• In order to solve the proposed ISAC optimization problem, two groups of approximate feasible domains are adopted to transform the optimization problem into convex.

• Finally, simulation results are provided to demonstrate the advantages and the effectiveness of the proposed symbol-scaling based CI-SLP design in ISAC systems.

II. System Model and Preliminaries

A. System Model

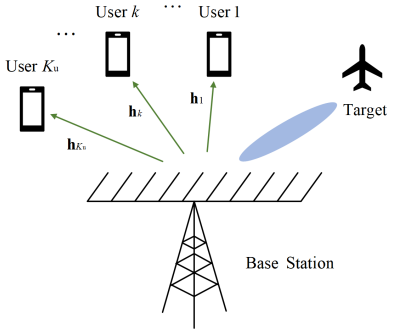

Fig. 1. The ISAC system with one multi-antenna ISAC BS serving multiple communication users while sensing the target of interest.

We consider a MIMO ISAC system as shown in Fig.1, where the multi-antenna ISAC BS simultaneously transmits radar probing waveforms to the target and communication symbols to the downlink users. The ISAC BS is equipped with a uniform linear array (ULA) of N antennas, serving K_{u} single-antenna users while detecting the target of interest at the same time, generally with $K_{\mathrm{u}} \leq N$. The same antenna array is used for both transmitting and receiving in different time slots via time-division (TD) protocol.

In this paper, the transmit signal matrix $\mathbf{X} = [\mathbf{x}[1], \mathbf{x}[2], \cdots, \mathbf{x}[L]] \in \mathbb{C}^{N\times L}$ is used as the ISAC waveform for both radar and communication operations, where $\mathbf{x}[l] = [x_1[l], x_2[l], \cdots, x_N[l]]^{\mathrm{T}} \in \mathbb{C}^{N\times 1}$ is the corresponding ISAC waveform in the l-slot with $l \in \{1, 2, \cdots, L\}$. In addition, the data symbol vector for K_{u} users in the l-th slot is denoted by $\mathbf{s}[l] = [s_1[l], s_2[l], \cdots, s_{K_{\mathrm{u}}}[l]]^{\mathrm{T}} \in \mathbb{C}^{K_{\mathrm{u}}\times 1}$, which is assumed to be drawn from a unit-norm PSK constellation. Unlike conventional BLP designs where $\mathbf{x}[l]$ is a linear function of $\mathbf{s}[l]$, SLP in general employs a non-linear mapping from $\mathbf{s}[l]$ to $\mathbf{x}[l]$, and optimizes $\mathbf{x}[l]$ directly according to the instantaneous symbol vector $\mathbf{s}[l]$ instead of using second-order statistics-based metrics.

B. Communication Model

The received signal for the k-th user in the l-th slot is

$$y_k[l] = \mathbf{h}_k^{\mathrm{T}}\mathbf{x}[l] + z_k^{\mathrm{c}}[l], \tag{1}$$

where $\mathbf{h}_k \in \mathbb{C}^{N\times 1}$ is the channel between the ISAC BS and user k, and $z_k^{\mathrm{c}}[l] \sim \mathcal{CN}(0, \sigma_{\mathrm{c}}^2)$ is the additive noise of user k in the l-th slot with σ_{c}^2 being the noise power.

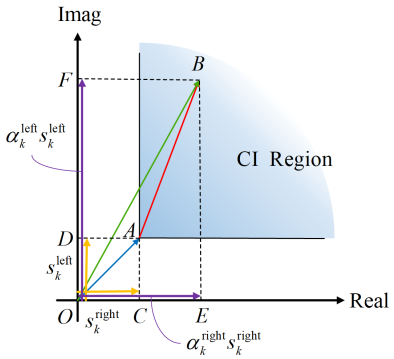

Fig. 2. Geometric diagram of the symbol-scaling CI metric for QPSK.

To illustrate the symbol-scaling CI meric introduced in [12], we depict one quarter of a QPSK constellation in Fig. 2 as an example, where we drop the time slot index $[l]$ for conciseness. Without loss of generality, we assume that $\overrightarrow{OA}$ is the nominal constellation point for user $k \in \{1, 2, \cdots, K\}$ in the l-th slot, i.e.,

$$\overrightarrow{OA} = s_k[l]. \tag{2}$$

$\overrightarrow{OB}$ represents the noiseless received signal with interference, which can be expressed as

$$\overrightarrow{OB} = \overrightarrow{OA} + \overrightarrow{AB} = \mathbf{h}_k^{\mathrm{T}}\mathbf{x}[l], \tag{3}$$

based on the geometry, and $\overrightarrow{AB}$ can be regarded as the sum CI from other user streams.

Different from the common phase-rotation CI metric which uses phase relations for SLP [13]–[15], we try to leverage the the symbol-scaling CI metric for SLP, which decomposes the signal along the decision boundaries and imposes scaling constraints on the decomposed components. One of the advantages for the symbol-scaling based SLP method is that the precoding optimization problem based on symbol scaling can be easily extended to QAM modulation [16]. Hence, we leverage the symbol-scaling metric to design the SLP scheme for enhancing the system ISAC performance.

Based on the symbol-scaling metric, $\overrightarrow{OA}$ is decomposed along the two decision boundaries of the QPSK modulation to obtain $\overrightarrow{OC}$ and $\overrightarrow{OD}$:

$$\begin{aligned}\overrightarrow{OA} &= \overrightarrow{OC} + \overrightarrow{OD} \\ &= s_k^{\text{right}}[l] + s_k^{\text{left}}[l].\end{aligned} \tag{4}$$

Following a similar procedure, the noiseless received signal $\overrightarrow{OB}$ can also be decomposed along the two decision boundaries as

$$\begin{aligned}\overrightarrow{OB} &= \overrightarrow{OE} + \overrightarrow{OF} \\ &= \alpha_k^{\text{right}}[l]\, s_k^{\text{right}}[l] + \alpha_k^{\text{left}}[l]\, s_k^{\text{left}}[l],\end{aligned} \tag{5}$$

where $\alpha_k^{\text{right}}[l]$ and $\alpha_k^{\text{left}}[l]$ are non-negative scaling factors. We can observe that the value of α_k^{right} or α_k^{left} represents the effect of inter-user CI, and a larger value of α_k^{right} or α_k^{left} means that the symbol can be pushed further away from one of its decision boundary.

By following the transformations in [17], we can construct a coefficient matrix $\mathbf{M} \in \mathbb{R}^{2K_{\text{u}} \times 2N}$ and obtain:

$$\boldsymbol{\alpha}_{\text{E}} = \mathbf{M}\mathbf{x}_{\text{E}}, \tag{6}$$

where $\boldsymbol{\alpha}_{\text{E}} \in \mathbb{R}^{2K_{\text{u}} \times 1}$ and $\mathbf{x}_{\text{E}} \in \mathbb{R}^{2N \times 1}$ are defined as

$$\begin{aligned}\boldsymbol{\alpha}_{\text{E}} &= \left[\alpha_1^{\text{right}}[l], \cdots, \alpha_{K_{\text{u}}}^{\text{right}}[l], \alpha_1^{\text{left}}[l], \cdots, \alpha_{K_{\text{u}}}^{\text{left}}[l]\right]^{\text{T}}, \\ \mathbf{x}_{\text{E}} &= \left[\Re\left(\mathbf{x}[l]\right)^{\text{T}}, \Im\left(\mathbf{x}[l]\right)^{\text{T}}\right]^{\text{T}}.\end{aligned} \tag{7}$$

The construction of $\mathbf{M}$ follows Section IV-A of [17].

C. Radar Model

For the radar sensing, the received signal at the target of interest is expressed as

$$r[l] = \beta \mathbf{a}(\theta)^{\text{H}} \mathbf{x}[l] + z^{\text{r}}[l], \tag{8}$$

where $\mathbf{a}(\theta) = \left[1, e^{j\sin\theta}, \cdots, e^{j(N-1)\sin\theta}\right]^{\text{T}} \in \mathbb{C}^{N \times 1}$ is the steering vector of the BS towards the target with θ as the corresponding azimuth angle. β accounts for the effective channel propagation coefficient, and $z^{\text{r}}[l] \sim \mathcal{CN}\left(0, \sigma_{\text{r}}^2\right)$ is the additive noise of the target in the l-th slot. Thus, the illumination power [18] towards the target is given by

$$\begin{aligned}P_{\text{r}} =& \beta^2 \cdot \left|\mathbf{a}(\theta)^{\text{H}} \mathbf{x}[l]\right|^2 \\ =& \beta^2 \left(\left|\mathbf{a}_{\text{E}}^{\text{T}} \mathbf{x}_{\text{E}}\right|^2 + \left|\mathbf{b}_{\text{E}}^{\text{T}} \mathbf{x}_{\text{E}}\right|^2\right),\end{aligned} \tag{9}$$

where $\mathbf{a}_{\text{E}} \in \mathbb{C}^{2N \times 1}$ and $\mathbf{b}_{\text{E}} \in \mathbb{C}^{2N \times 1}$ are defined as

$$\begin{aligned}\mathbf{a}_{\text{E}} &= \left[\Re\left(\mathbf{a}(\theta)\right)^{\text{T}}, \Im\left(\mathbf{a}(\theta)\right)^{\text{T}}\right]^{\text{T}}, \\ \mathbf{b}_{\text{E}} &= \left[-\Im\left(\mathbf{a}(\theta)\right)^{\text{T}}, \Re\left(\mathbf{a}(\theta)\right)^{\text{T}}\right]^{\text{T}}.\end{aligned} \tag{10}$$

The radar illumination power is expected to be no less than a preset minimum to guarantee the detection probabilities. Hence the radar constraint is formulated as

$$\beta^2 \left(\left|\mathbf{a}_{\text{E}}^{\text{T}} \mathbf{x}_{\text{E}}\right|^2 + \left|\mathbf{b}_{\text{E}}^{\text{T}} \mathbf{x}_{\text{E}}\right|^2\right) \geq p_{\text{r}}, \tag{11}$$

where $p_{\text{r}} > 0$ is the preset minimum illumination power requirement for the target.

III. Symbol-Scaling CI-SLP Design for ISAC

A. Problem Formulation

Based on the above description, in this paper, we aim to design the transmit signal vector $\mathbf{x}_{\text{E}}$ to maximize the minimum entry in $\boldsymbol{\alpha}_{\text{E}}$ so as to enhance the overall communication performance during the considered time period. As for the radar sensing performance, we introduce the the illumination power requirement for the target and total power budget constraint. Therefore, the SLP optimization problem for ISAC is formulated as

$$\mathcal{P}_0: \max_{\mathbf{x}_{\text{E}}} \min_{i} \alpha_i \tag{12}$$

$$\text{s.t.} \quad \boldsymbol{\alpha}_{\text{E}} = \mathbf{M}\mathbf{x}_{\text{E}}, \tag{12a}$$

$$\beta^2 \left(\left|\mathbf{a}_{\text{E}}^{\text{T}} \mathbf{x}_{\text{E}}\right|^2 + \left|\mathbf{b}_{\text{E}}^{\text{T}} \mathbf{x}_{\text{E}}\right|^2\right) \geq p_{\text{r}}, \tag{12b}$$

$$\|\mathbf{x}_{\text{E}}\|_2^2 \leq p_0, \tag{12c}$$

where α_i represents the i-th entry in $\boldsymbol{\alpha}_{\text{E}}$, and p_0 represents the transmit power budget per symbol slot.

We note that the total power constraint (12c) can be extended to other power-related constraints, such as the following per-antenna power constraint

$$\left|x_{\text{E},n}\right|^2 + \left|x_{\text{E},n+N}\right|^2 \leq \frac{p_0}{N}, \ \forall n \in \{1, \cdots, N\}, \tag{13}$$

which is also a convex constraint. Here, $x_{\text{E},n}$ represents the n-th entry in $\mathbf{x}_{\text{E}}$.

$\mathcal{P}_0$ is non-convex because the constraint on the target illumination power (12b) is non-convex. Therefore, we first deal with the constraint of the target illumination power.

B. Problem Transformation

By defining $\hat{p}_{\text{r}} = \frac{p_{\text{r}}}{\beta^2}$, $r_1 = \mathbf{a}_{\text{E}}^{\text{T}} \mathbf{x}_{\text{E}}$ and $r_2 = \mathbf{b}_{\text{E}}^{\text{T}} \mathbf{x}_{\text{E}}$, the constraint on the target illumination power constraint (12b) can be written as:

$$r_1^2 + r_2^2 \geq \hat{p}_{\text{r}}. \tag{14}$$

This constraint indicates that the feasible solutions of r_1 and r_2 fall outside a circle shown in Fig. 3(a), which is a non-convex constraint. We try several tangent lines of the circle as its approximations, so as to transform the non-convex constraint into convex. As shown in Fig. 3(b) and 3(c), we select two groups of approximate feasible domains, which are given below:

1) The first group has four tangent lines, and the approximated feasible region includes four convex sets which is given below

$$\begin{aligned}&\mathbb{S}_1 = \mathbb{T}_1 \cup \mathbb{T}_2, \\ &\mathbb{T}_1 = \left\{\mathbf{x}_{\text{E}} | r_1 \leq -\sqrt{\hat{p}_{\text{r}}}\right\} \cup \left\{\mathbf{x}_{\text{E}} | r_1 \geq \sqrt{\hat{p}_{\text{r}}}\right\}, \\ &\mathbb{T}_2 = \left\{\mathbf{x}_{\text{E}} | r_2 \leq -\sqrt{\hat{p}_{\text{r}}}\right\} \cup \left\{\mathbf{x}_{\text{E}} | r_2 \geq \sqrt{\hat{p}_{\text{r}}}\right\}.\end{aligned} \tag{15}$$

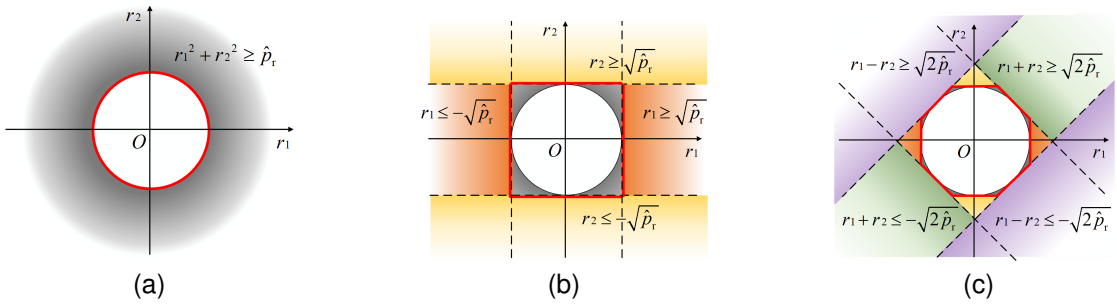

Fig. 3. (a) The constraint on the target illumination power. (b) The first group of feasible domains. (c) The second group of feasible domains.

2) The second group has eight tangent lines, and the approximated feasible region includes eight convex sets which is given below

$$\begin{aligned}&\mathbb{S}_2=\mathbb{S}_1\cup\mathbb{T}_3\cup\mathbb{T}_4,\\&\mathbb{T}_3=\left\{\mathbf{x}_\mathrm{E}|r_1+r_2\leq-\sqrt{2\hat{p}_\mathrm{r}}\right\}\cup\left\{\mathbf{x}_\mathrm{E}|r_1+r_2\geq\sqrt{2\hat{p}_\mathrm{r}}\right\},\\&\mathbb{T}_4=\left\{\mathbf{x}_\mathrm{E}|r_1-r_2\leq-\sqrt{2\hat{p}_\mathrm{r}}\right\}\cup\left\{\mathbf{x}_\mathrm{E}|r_1-r_2\geq\sqrt{2\hat{p}_\mathrm{r}}\right\}.\end{aligned}\tag{16}$$

It is easy to note that the above two groups of feasible domains are all unions of some simple convex sets. Therefore, the solution of the original optimization problem $\mathcal{P}_0$ can be easily transformed into solving several convex optimization problems. Note that the approximated problem with the second group of feasible domains has smaller gap with problem $\mathcal{P}_0$, but the corresponding complexity is higher compared with the first group, which will be confirmed in Section VI. Through choosing different groups can achieve different trade-offs between the ISAC performance and computational complexity. It is true that we can further increase the number of tangent lines to get more accurate approximation but at the sacrifice of higher complexity.

Specifically, these convex optimization problems corresponding to different convex sets can be written in a unified form:

$$\mathcal{P}_1:\ \max_{\mathbf{x}_\mathrm{E}}\ \min_{i}\ \alpha_i\tag{17}$$
$$\text{s.t.}\ \ \boldsymbol{\alpha}_\mathrm{E}=\mathbf{M}\mathbf{x}_\mathrm{E},\tag{17a}$$
$$\mathbf{c}^\mathrm{T}\mathbf{x}_\mathrm{E}\geq d,\tag{17b}$$
$$\|\mathbf{x}_\mathrm{E}\|_2^2\leq p_0,\tag{17c}$$

where $\mathbf{c}$ and d in (17b) take different values according to different convex sets.

Further, we can equivalently transform problem $\mathcal{P}_1$ to the following minimization problem $\mathcal{P}_2$ by introducing an auxiliary variable t

$$\mathcal{P}_2:\ \min_{t,\mathbf{x}_\mathrm{E}}\ -t\tag{18}$$
$$\text{s.t.}\ \ \mathbf{M}\mathbf{x}_\mathrm{E}\geq t\cdot\mathbf{1},\tag{18a}$$
$$\mathbf{c}^\mathrm{T}\mathbf{x}_\mathrm{E}\geq d,\tag{18b}$$
$$\|\mathbf{x}_\mathrm{E}\|_2^2\leq p_0.\tag{18c}$$

It is easy to prove that $\mathcal{P}_2$ is a standard convex optimization problem that can be directly solved via optimization tools such as CVX [19]. Furthermore, $\mathcal{P}_2$ can be solved more efficiently with the aid of the modified Hook-Jeeves Pattern Search algorithm [20].

Therefore, for each group of feasible domains, we just need to solve the optimization problem $\mathcal{P}_2$ individually under certain convex set with specific $\mathbf{c}$ and d to get sets of local optimal solutions to the original optimization problem $\mathcal{P}_0$, and then we choose the solution with the best result among these sets of local optimal solutions as the global optimal solution. In particular, assuming that the number of $\mathcal{P}_2$ to be solved is N_p, then N_p sets of local optimal solutions will be obtained. For example, $N_\mathrm{p}=4$ and 8 for the first and second of feasible domains, respectively. By denoting these N_p sets of local optimal solutions as $\left\{\left\{t_1^*,\mathbf{x}_{\mathrm{E},1}^*\right\},\cdots,\left\{t_{N_\mathrm{p}}^*,\mathbf{x}_{\mathrm{E},N_\mathrm{p}}^*\right\}\right\}$, then the global optimal solution $\mathbf{x}_\mathrm{E}^*=\mathbf{x}_{\mathrm{E},n}^*$ can be determined as follows:

$$n=\underset{i=\{1,\cdots,N_\mathrm{p}\}}{\operatorname{argmax}}\ t_i^*.\tag{19}$$

Finally, the optimal transmit signal vector in the l-slot can be obtained:

$$\mathbf{x}[l]=\begin{bmatrix}\mathbf{I}_N & \mathbf{O}_N\end{bmatrix}\cdot\mathbf{x}_\mathrm{E}^*+j\cdot\begin{bmatrix}\mathbf{O}_N & \mathbf{I}_N\end{bmatrix}\cdot\mathbf{x}_\mathrm{E}^*,\tag{20}$$

based on the definition of $\mathbf{x}_\mathrm{E}$ in (7). The proposed symbol-scaling CI-SLP design for ISAC in this section can be summarized by the following Algorithm 1.

Algorithm 1 Symbol-Scaling CI-SLP Design for ISAC

1: **Input**: $\mathbf{s}_k[l]$, $\mathbf{H}=[\mathbf{h}_1,\cdots,\mathbf{h}_{K_\mathrm{u}}]^\mathrm{T}$, $\mathbf{a}(\theta)$, p_0, $\hat{p}_\mathrm{r}$
2: Initial $\mathbf{M}$, $\mathbf{a}_\mathrm{E}$ and $\mathbf{b}_\mathrm{E}$;
3: Solve N_p optimization problems $\mathcal{P}_2$, with specific $\mathbf{c}$ and d according to the composition of the feasible domain and obtain $\left\{\left\{t_1^*,\mathbf{x}_{\mathrm{E},1}^*\right\},\cdots,\left\{t_{N_\mathrm{p}}^*,\mathbf{x}_{\mathrm{E},N_\mathrm{p}}^*\right\}\right\}$;
4: Find the global optimal solution $\mathbf{x}_\mathrm{E}^*$ by (19);
5: Obtain the transmit signal vector $\mathbf{x}[l]$ by (20).
6: **Output**: $\mathbf{x}[l]$

IV. Simulation Results

In this section, we present numerical results to validate the above derivations and illustrate the superiority of the proposed

approach. The proposed schemes are compared with PDD-MM-BCD in [13] in terms of SER performance, transmit beampattern and execution time. The execution time results are obtained from a Windows 11 Desktop with i5-12400 and 16GB RAM.

The following abbreviations are used throughout this section:

1) PDD-MM-BCD: PDD-MM-BCD in [13], which is an CI-SLP scheme based on the penalty dual decomposition (PDD), majorization-minimization (MM), and block coordinate descent (BCD) methods for ISAC system.
2) ISAC-SS-SLP(1/2): The proposed CI-SLP based on symbol scaling summarized in Algorithm 1, with the first/second group of feasible domains.

Throughout the simulations, the transmit power budget per symbol slot is set as $p_0 = 30$dBm, and QPSK modulation is employed. The BS is equipped with N antennas with antenna spacing $\Delta = \frac{\lambda}{2}$ where λ is the wavelength of the carrier signal. We set the QoS for communication requirement of the PDD-MM-BCD scheme as $\beta_c = \sigma_c\Gamma_c$, where $\sigma_c = 22$dBm and $\Gamma_c = 2.2$dB . In the ISAC-SS-SLP scheme proposed in this paper, we assume that the illumination power requirement for the target is $p_r = \sigma_r\Gamma_r$, where $\Gamma_r = 18.4$dB and $\sigma_r = 20$dBm.

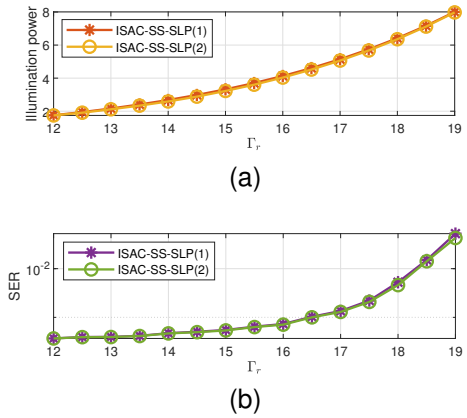

Fig. 4. The effect of Γ_r on the ISAC-SS-SLP scheme, $N = 10$, $K_u = 3$. (a) illumination power towards the target versus Γ_r. (b) SER versus Γ_r

The effect of Γ_r on the ISAC-SS-SLP scheme is first plotted, when $N = 10$, $K_u = 3$, and the target at the location $\theta_1 = 0°$ with $\beta_1 = 1$. In Fig. 4(a) and 4(b), a larger Γ_r means a higher requirement for illumination power towards the target, and at the same time the SER performance for communication will be worse.

Fig. 5(a) and 5(b) respectively depict the SER performance and transmit beampatterns of different schemes, when $N = 10$, $K_u = 3$, and the target at the location $\theta_1 = 0°$ with $\beta_1 = 1$. When the transmit beampatterns are similar, the proposed CI-SLP ISAC schemes based on symbol scaling can obtain better SER performance under the constraint of the second group of feasible domains, because the second group of feasible domains is closer to the original feasible domains. ISAC-SS-SLP constrained by the first and the second groups of feasible

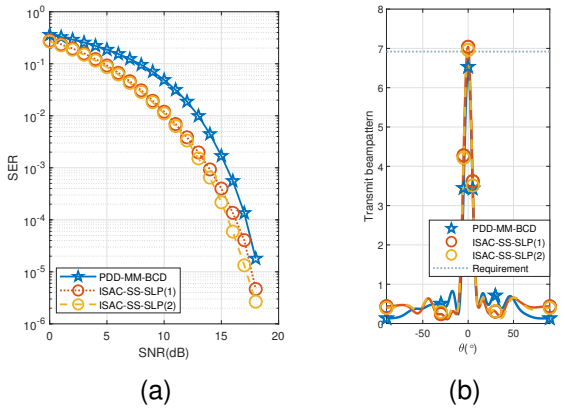

Fig. 5. Transmit Beampatterns of different schemes, $N = 10$, $K_u = 3$. (a) SER performance. (b) Transmit Beampattern.

domains can achieve better SER performance than PDD-MM-BCD, which shows the advantages of our proposed CI-SLP ISAC schemes based on symbol scaling. For ISAC-SS-SLP, the results of taking the first and the second groups of feasible domains are very close, indicating that these two groups of feasible domains are closely approaching the original non-convex feasible domains.

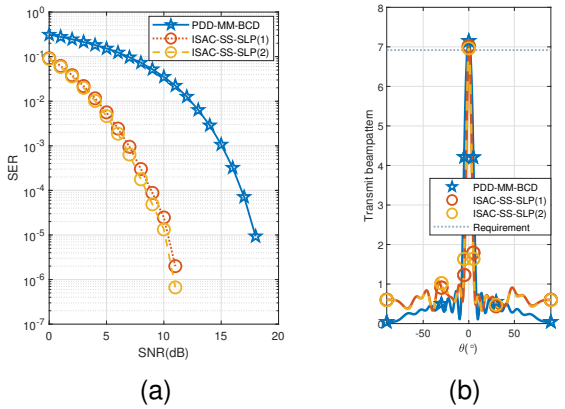

Fig. 6. Performance of different schemes, $N = 15$, $K_u = 3$. (a) SER performance. (b) Transmit Beampattern.

Fig. 6(a) and 6(b) respectively depict the SER performance and transmit beampatterns of different schemes, when $N = 15$, $K_u = 3$, and the target at the location $\theta_1 = 0°$ with $\beta_1 = 1$. At this time with a larger number of transmit antennas, although the sidelobe power of PDD-MM-BCD is decreased, the illumination power in the target direction is not significantly improved. This indicates that the performance improvement of PDD-MM-BCD by increasing the number of transmit antennas is limited. At the same time, it can be observed that the SER performance of the proposed SLP ISAC schemes based on symbol scaling is greatly improved when the number of transmit antennas increases, i.e., a 7dB SNR reduction can be obtained when achieving the same SER

performance with PDD-MM-BCD scheme, which means that our proposed scheme is more potential in massive MIMO systems.

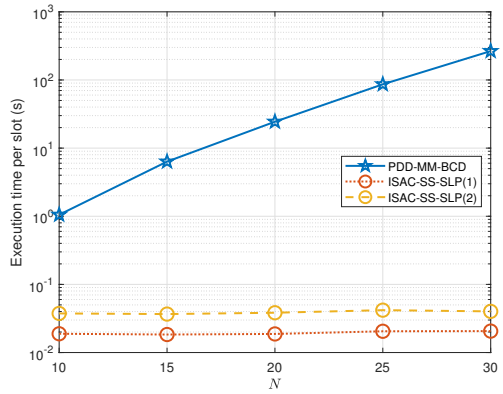

Fig. 7. SER performance of different schemes, $N = 10$, $K_u = 3$.

Fig. 7 depicts the complexity of the proposed schemes with PDD-MM-BCD in terms of the execution time. For fairness of comparison, the optimization problems in PDD-MM-BCD and ISAC-SS-SLP are solved by the Hooked-Jeeves pattern search algorithm. With the increase of the number of transmit antennas, the computational complexity of each scheme will increase correspondingly, because the number of optimization variables in the optimization problem increases. As can be seen, the execution time of CI-SLP ISAC schemes based on symbol scaling is significantly less than PDD-MM-BCD, thanks to the objective function in the original problem that does not require approximation, which eliminates the need for iterative procedures.

V. Conclusion

In this work, we propose a symbol-scaling based CI-SLP design in ISAC system. The minimum communication scaling factor among the communication users is maximized while satisfying the radar target illumination power requirement and total power budget constraint. In order to solve the proposed ISAC optimization problem, two groups of approximate feasible domains are adopted to transform the optimization problem into convex. simulation results are provided to demonstrate the advantages and the effectiveness of the proposed symbol-scaling based CI-SLP design in ISAC systems.

Acknowledgement

This work is partially supported by the National Natural Science Foundation of China under Grant 62201449, the Key R&D Projects of Shaanxi Province under Grant 2023-YBGY-040, the Qin Chuang Yuan High-Level Innovation, the Entrepreneurship Talent Program under Grant QCYRCXM-2022-231, anf the “Si Yuan Scholar” Foundation.

References

[1] J. A. Zhang, M. L. Rahman, K. Wu, X. Huang, Y. J. Guo, S. Chen, and J. Yuan, “Enabling Joint Communication and Radar Sensing in Mobile Networks—A Survey,” *IEEE Commun. Surveys Tuts.*, vol. 24, no. 1, pp. 306–345, 2022.

[2] F. Liu, Y. Cui, C. Masouros, J. Xu, T. X. Han, Y. C. Eldar, and S. Buzzi, “Integrated Sensing and Communications: Toward Dual-Functional Wireless Networks for 6G and Beyond,” *IEEE J. Sel. Areas Commun.*, vol. 40, no. 6, pp. 1728–1767, 2022.

[3] D. Ma, N. Shlezinger, T. Huang, Y. Liu, and Y. C. Eldar, “Joint Radar-Communication Strategies for Autonomous Vehicles: Combining Two Key Automotive Technologies,” *IEEE Signal Process. Mag.*, vol. 37, no. 4, pp. 85–97, 2020.

[4] P. Kumari, S. A. Vorobyov, and R. W. Heath, “Adaptive Virtual Waveform Design for Millimeter-Wave Joint Communication–Radar,” *IEEE Trans. Signal Process.*, vol. 68, pp. 715–730, 2020.

[5] X. Hu, C. Masouros, F. Liu, and R. Nissel, “Low-PAPR DFRC MIMO-OFDM Waveform Design for Integrated Sensing and Communications,” in *IEEE International Conference on Communications (ICC)*, 2022, pp. 1599–1604.

[6] F. Liu, C. Masouros, A. Li, H. Sun, and L. Hanzo, “MU-MIMO Communications With MIMO Radar: From Co-Existence to Joint Transmission,” *IEEE Trans. Wireless Commun.*, vol. 17, no. 4, pp. 2755–2770, 2018.

[7] Z. Cheng, B. Liao, and Z. He, “Hybrid Transceiver Design for Dual-Functional Radar-Communication System,” in *2020 IEEE 11th Sensor Array and Multichannel Signal Processing Workshop (SAM)*, Hangzhou, China, 2020, pp. 1–5.

[8] C. Xu, B. Clerckx, and J. Zhang, “Multi-Antenna Joint Radar and Communications: Precoder Optimization and Weighted Sum-Rate vs Probing Power Tradeoff,” *IEEE Access*, vol. 8, pp. 173 974–173 982, 2020.

[9] X. Hu, C. Masouros, F. Liu, and R. Nissel, “MIMO-OFDM dual-functional radar-communication systems: Low-PAPR waveform design,” *arXiv preprint arXiv:2109.13148*, 2021.

[10] X. Liu, T. Huang, N. Shlezinger, Y. Liu, J. Zhou, and Y. C. Eldar, “Joint Transmit Beamforming for Multiuser MIMO Communications and MIMO Radar,” *IEEE Trans. Signal Process.*, vol. 68, pp. 3929–3944, 2020.

[11] J. Li and P. Stoica, “MIMO Radar with Colocated Antennas,” *IEEE Signal Process. Mag.*, vol. 24, no. 5, pp. 106–114, 2007.

[12] A. Li, D. Spano, J. Krivochiza, S. Domouchtsidis, C. G. Tsinos, C. Masouros, S. Chatzinotas, Y. Li, B. Vucetic, and B. Ottersten, “A Tutorial on Interference Exploitation via Symbol-Level Precoding: Overview, State-of-the-Art and Future Directions,” *IEEE Commun. Surveys Tuts.*, vol. 22, no. 2, pp. 796–839, Mar. 2020.

[13] R. Liu, M. Li, Q. Liu, and A. L. Swindlehurst, “Dual-Functional Radar-Communication Waveform Design: A Symbol-Level Precoding Approach,” *IEEE J. Sel. Topics Signal Process.*, vol. 15, no. 6, pp. 1316–1331, 2021.

[14] R. Liu, M. Li, Q. Liu, and A. L. Swindlehurst, “Joint Waveform and Filter Designs for STAP-SLP-Based MIMO-DFRC Systems,” *IEEE J. Sel. Areas Commun.*, vol. 40, no. 6, pp. 1918–1931, 2022.

[15] P. Li, Z. Xiao, M. Li, R. Liu, and Q. Liu, “Low-Range-Sidelobe Waveform Design for MIMO-OFDM ISAC Systems,” 2023. [Online]. Available: https://arxiv.org/abs/2305.18847.

[16] A. Li, C. Masouros, B. Vucetic, Y. Li, and A. L. Swindlehurst, “Interference Exploitation Precoding for Multi-Level Modulations: Closed-Form Solutions,” *IEEE Trans. Commun.*, vol. 69, no. 1, pp. 291–308, 2021.

[17] A. Li, C. Masouros, F. Liu, and A. L. Swindlehurst, “Massive MIMO 1-Bit DAC Transmission: A Low-Complexity Symbol Scaling Approach,” *IEEE Trans. Wireless Commun.*, vol. 17, no. 11, pp. 7559–7575, Nov. 2018.

[18] L. Wu, B. Wang, Z. Cheng, B. S. M. R, and B. Ottersten, “Joint Symbol-Level Precoding and Sub-Block-Level RIS Design for Dual-Function Radar-Communications,” in *2023 IEEE International Conference on Acoustics, Speech and Signal Processing (ICASSP)*, Rhodes Island, Greece, 2023, pp. 1–5.

[19] S. Boyd and L. Vandenberghe, *Convex Optimization*. Cambridge University Press, 2004.

[20] R. Liu, M. Li, Q. Liu, and A. L. Swindlehurst, “Secure Symbol-Level Precoding in MU-MISO Wiretap Systems,” *IEEE Transactions on Information Forensics and Security*, vol. 15, pp. 3359–3373, 2020.